J. Fluid Mech. (1973), *vol.* 57, *part* 3, *pp.* 491–514
Printed in Great Britain

Bounds for heat transport in a porous layer

By V. P. GUPTA† AND D. D. JOSEPH
Department of Aerospace Engineering and Mechanics, University of Minnesota

(Received 17 August 1972)

Strongly nonlinear heat transport across a porous layer is studied using Howard's (1963) variational method. The analysis explores a bifurcation property of Busse's (1969) multi-α solution of this variational problem and complements the 1972 study of Busse & Joseph by further restricting the fields which are allowed to compete for the maximum heat transported at a given temperature difference. The restriction arises, as in the case of infinite Prandtl number convection studied by Chan (1971), from letting a parameter tend to infinity from the outset; here, however, the parameter which is assumed infinitely large (the Prandtl–Darcy number) is actually seldom smaller than $O(10^7)$.

The theoretical bounding heat-transport curve is computed numerically. The maximizing Nusselt number (Nu) curve is given at first by a functional of the single-α solution; then this solution bifurcates and the Nusselt number functional is maximized for an interval of Rayleigh numbers (R) by the two-α solution. The agreement between the numerical analysis and recent experiments is striking. The theoretical heat-transport curve is found to be continuously differentiable but has piecewise discontinuous second derivatives.

The results of an asymptotic ($R \to \infty$) analysis following Chan (1971) are in qualitative agreement with the results of numerical analysis and give the asymptotic law $Nu = 0{\cdot}016R$. This law is consistent with the result of the porous version of the well-known dimensional argument leading to the one-third power law for regular convection. The asymptotic results, however, do not appear to be in good quantitative agreement with the numerical results.

1. Introduction

The objective of the bounding theory of turbulence is to provide bounds on average properties of statistically stationary turbulent flows. The average properties are regarded as functionals of the turbulent velocity field which can be defined for more general vector fields. The bounds are derived by determining the extremum of the functional among a class of vector fields which includes all statistically stationary solutions of the basic equations of motion. By restricting the fields admitted into competition for the extremum to those which share with the solutions an ever greater number of properties, one can improve the bounds and bring them into ever closer correspondence with the observed values.

Howard (1963), following earlier ideas of Malkus (1954*b*), was the first to use

† Present address: The Mitre Corporation, McLean, Virginia 22101, U.S.A.

this approach when he derived upper bounds for the heat transport by convection in a fluid layer heated from below.

Busse, in 1969, made an important contribution towards the solution of the problem posed by Howard. He suggested that the extremalizing solutions should have increasingly smaller 'scales' introduced as the intensity of the turbulence increases. He called these solutions multi-α solutions and studied them by boundary-layer methods. The boundary-layer analysis of the multi-α solutions rested on a number of unproven assumptions. These assumptions are most easily examined in the context of porous convection (Busse & Joseph 1972, hereafter called BJ) since this is possibly the simplest of natural configurations in which multi-α solutions occur. The analysis of porous convection allows one to characterize the multi-α solutions through 'orthogonality' relations in which the wavenumbers play the role of eigenvalues, and to prove a number of results about the solution. Moreover, the simplicity of the problem of porous convection allowed for the first time the numerical calculation of the two-α solution by a Galerkin method. The analysis confirms the essential validity of the boundary-layer solutions.

The boundary-layer analysis, however, is misleading in certain very important details of the solution. In particular, the boundary-layer solutions lead to definite 'breaks' in the slope of the heat-transport curve. The more exact analysis of BJ, and the analysis given here, indicates that the appearance of solutions with ever more wavenumbers is a bifurcation phenomenon: for a certain range of Rayleigh numbers the heat transported is maximized by a solution with N wavenumbers. At a critical value of R, a new solution with $N+1$ wavenumbers differing infinitesimally from the N-wavenumber solution becomes possible and maximizes the heat transport. The bifurcation process implies that the bounding heat-transport curve is a smooth curve having breaks in curvature rather than slope (the bounding heat-transport curve is continuously differentiable with piecewise continuous second derivatives).†

The results of the variational analysis given in BJ are in good agreement with experiments in a range of Rayleigh numbers up to about $11\pi^2$ ($\sim 2{\cdot}5R_c$). At higher Rayleigh numbers, however, the appearance of maximizing solutions with many wavenumbers drives the bounding heat-transport curve away from the observed data.

Motivating the present study is the observation that the form of the flow of liquids in naturally permeable materials results through a balance of the Darcy resistance against externally imposed pressure gradients and body forces. In other words, the inertial force terms in the momentum equation are negligible compared with the other terms. In terms of dimensionless parameters for flows driven by temperature differences, this implies a limit of infinite Prandtl–Darcy number ($B^{-1} \to \infty$). As in the infinite Prandtl number problem of regular convection which was treated recently by Chan (1971), the $B \to 0$ limit linearizes the momentum equation and allows one to formulate the variational problem for the

† Bifurcation from conduction to convection is an exception in this regard. Here we have a break in slope. But all further bifurcations cause a jump in curvature of the heat-transport curve.

heat transport as an integral consequence of the heat equation with the momentum equation as a pointwise-valid differential-equation side constraint.

It goes without saying that the constrained maximum problem will lead to smaller values of the heat transport. What is really noteworthy, however, is the degree to which the solutions of the constrained variational problem seem to correspond to the observed physics. The agreement between the bounding heat-transport curves and the ones which were observed by Combarnous & LeFur (1969), and more recently by Buretta & Berman (1973), is particularly striking. In these experiments one observes a change in the slope of the heat-transport curve which is sometimes regarded, with insufficient evidence, as a 'break' in the slope of the heat-transport curve. Such qualitative changes in the shape of the heat-transport curve were first observed for the Bénard problem by Schmidt & Saunders (1938) and their significance was first recognized by Malkus (1954*a*). The same qualitative changes evidently are true for porous convection. Our exact numerical analysis of the constrained variational problem for the heat transport is in splendid agreement with Buretta & Berman's (1973) observations for the entire range of Rayleigh numbers which we computed. In particular, the point at which the two-α solution bifurcates from the single-α solution is in good agreement with the observed changes in the shape of the heat-transport curve.

Having made this case for agreement of theory with experiment we must caution that 'upper bounds' would be expected to coincide with the heat-transport curve only if the solutions of the Darcy–Oberbeck–Boussinesq equations were to coincide with solutions of the Euler equations for the maximum value of the heat-transport functional. It should be possible to integrate the DOB equations for roll convection numerically and to compare these exact results with the results of the variational analysis given here.

The basis for our exact numerical analysis is not really new, though it appears that this is the first successful direct numerical integration of the Euler equations for the bounding problem. The technique used here is a standard quasi-linearization of the governing Euler equations coupled with the use of Conte's orthonormalization method.

2. Formulation of the variational problem

The configuration to be considered is a horizontal porous layer of infinite extent filled with fluid and heated from below. The layer has thickness d and is bounded by two parallel plates. The upper plate is at a constant temperature T_1, the lower plate at temperature T_2. To obtain a dimensionless description of the problem, we shall use d, d^2/κ, $T_2 - T_1$ and κ/d as units of length, time, temperature and velocity, respectively.

It will be convenient and sufficient for our purpose to start the analysis with the dimensionless version of the Darcy–Oberbeck–Boussinesq (DOB) equations as set down by Lapwood (1948). We have

$$B(\mathbf{u}_t + \mathbf{u}\,.\,\nabla\mathbf{u}) + \nabla P - \mathbf{k}R(T - T_1) + \mathbf{u} = 0 \tag{2.1}$$

and

$$T_t + \mathbf{u}\,.\,\nabla T - \nabla^2 T = 0, \tag{2.2a}$$

where $$\operatorname{div}\mathbf{u} = 0, \quad \mathbf{u} = u_1\mathbf{i} + u_2\mathbf{j} + u_3\mathbf{k}. \tag{2.2b}$$

The boundary conditions are

$$T = 1, \quad u_3 = 0 \quad \text{at} \quad z = 0$$

and

$$T = 0, \quad u_3 = 0 \quad \text{at} \quad z = 1. \tag{2.2c}$$

Since the Darcy constitutive assumption has replaced the Newtonian stress divergence $\nabla^2\mathbf{u}$ with a resistance proportional to a Darcy averaged velocity $(-\mathbf{u})$ in the last term of (2.1), we cannot impose boundary conditions on the tangential components of the velocity vector.

The parameters of the problem (2.1*a*) are the Rayleigh number

$$R = \gamma g K d(T_2 - T_1)/\nu\kappa$$

and the Prandtl–Darcy number

$$B^{-1} = (\nu/\kappa)\,(d^2/K).$$

The constants γ, g, ν and K are the coefficient of thermal expansion, the acceleration due to gravity, the kinematic viscosity and the Darcy permeability coefficient, respectively. The thermal diffusivity κ is here the ratio of thermal conductivity of the fluid–solid mixture to products of the specific heat and density of the fluid.

The velocity $\mathbf{u}$ in (2.2) is the Darcy seepage velocity and not the actual velocity in the pores. Therefore the terms involving $\mathbf{u}\cdot\nabla\mathbf{u}$ need not be correct. Indeed experiments dating back to 1901 (Forchheimer 1901; Ward 1964; Beavers & Sparrow 1969) all give a drag proportional to the square of the average velocity in rectilinear flow. It has been suggested (cf. Irmay 1958) that the vector correction for weakly nonlinear porous flow should also take form in a quadratic drag proportional to $\mathbf{u}|\mathbf{u}|$.

The analysis of BJ assumed the Lapwood form (2.1) of the DOB equation. The purpose of that analysis was to expose and develop the variational method in its simplest mathematical context. The parameter B did not enter the analysis of BJ because the term involving $\mathbf{u}\cdot\nabla\mathbf{u}$ in the energy identities integrates to zero. The results of BJ therefore hold for all B.

The present analysis explores the consequences of assigning a particular value to B; the physically appropriate value $B = 0$ follows from extraordinarily small values of the permeability coefficient K in porous material: in sand, $K = O(10^{-8})$ cm^2; in very porous fibre metals, $K = O(10^{-4})$ cm^2. When $B = 0$ then

$$\nabla P - \mathbf{k}R(T - T_1) + \mathbf{u} = 0 \tag{2.2d}$$

is the appropriate form of the DOB equations independent of the form which is assumed for the nonlinear convection of Darcy's law. The fact that $B \to 0$ for natural materials means that thermally driven motion in porous material will ordinarily be very slow motion.

The goal of the following analysis is to obtain bounds on the heat transport by convection under statistically stationary conditions, i.e. we make the usual assumptions that the physically realized solutions of (2.1) and (2.2) are such that

their horizontal averages exist, are bounded, and are time-independent. Restricting our attention from now on to such solutions, we shall indicate the horizontal average by an overbar, and layer average by angular brackets:

$$\bar{f} = \bar{f}(z) = \lim_{L\to\infty}\left[\frac{1}{4L^2}\int_{-L}^{L}\int_{-L}^{L} f(x,y,z)\,dx\,dy\right]$$

and

$$\langle f\rangle = \int_0^1 \bar{f}(z)\,dz.$$

Thus, we can define the fluctuating temperature

$$T^* = T - \bar{T},$$

where

$$T^* = 0 \quad \text{at} \quad z = 0, 1. \tag{2.3a}$$

Taking the horizontal average of (2.2*b*), we show that

$$\bar{u}_3 = 0. \tag{2.3b}$$

Similarly, the horizontal average of (2.2*a*), using (2.2*b*) and (2.3*b*), gives

$$\frac{d}{dz}\overline{u_3 T} = \frac{d}{dz}\overline{u_3 T^*} = \frac{d^2\bar{T}}{dz^2}. \tag{2.4}$$

Integrating (2.4) and using boundary conditions (2.2*c*) and (2.3*a*) we get

$$\overline{u_3 T^*} - \frac{d\bar{T}}{dz} = 0 - \frac{d\bar{T}}{dz}\bigg|_{z=0}. \tag{2.5}$$

The layer average of (2.5) gives

$$-\frac{d\bar{T}}{dz}\bigg|_{z=0} = \langle u_3 T^*\rangle + 1 = Nu \equiv 1 + F, \tag{2.6}$$

where Nu is the Nusselt number. Combining (2.5) and (2.6) we get

$$\frac{d\bar{T}}{dz} = \overline{u_3 T^*} - 1 - \langle u_3 T^*\rangle. \tag{2.7}$$

Multiplying (2.2*a*) by T^* and averaging over the layer leads to

$$\left\langle \overline{u_3 T^*}\frac{d\bar{T}}{dz}\right\rangle = -\langle|\nabla T^*|^2\rangle. \tag{2.8}$$

Substituting $d\bar{T}/dz$ from (2.7) into (2.8) we find that

$$\langle u_3 T^*\rangle^2 - \langle\overline{u_3 T^*}^2\rangle + \langle u_3 T^*\rangle = \langle|\nabla T^*|^2\rangle. \tag{2.9a}$$

We can take the scalar product of (2.1) with $\mathbf{u}$, take its layer average and find that

$$\langle|\mathbf{u}|^2\rangle = R\langle u_3 T\rangle = R\langle u_3 T^*\rangle. \tag{2.9b}$$

The analysis of BJ defines the extremum problem for all solenoidal velocity and temperature fluctuation fields u_3 and T^* which satisfy the integral constraints (2.9*a*) and (2.9*b*).

In the present analysis we replace the integral side constraint (2.9 b) with the differential-equation side constraint

$$\nabla^2 u_3 - R\nabla_1^2 T^* = 0, \tag{2.9c}$$

where $\nabla_1^2 = \partial_{xx}^2 + \partial_{yy}^2$ is the horizontal Laplace operator. Equation (2.9 c) can be obtained as the vertical component of the double curl of (2.2 d). We note that, since $\mathbf{k} \cdot \operatorname{curl} \mathbf{u} = 0$ and $\mathbf{u}$ is solenoidal, $\mathbf{u}$ is a purely poloidal field which can be obtained from a potential χ according to the prescription

$$\mathbf{u} = -\operatorname{curl}^2 \mathbf{k}\chi. \tag{2.10}$$

Given a scalar field u_3 we may find χ and the other components of $\mathbf{u}$ from (2.10).

To complete the preliminaries for the statement of the variational problem, it is convenient to introduce the following changes of scale:

$$u_3 = bR^{\frac{1}{2}}w, \quad T^* = bR^{-\frac{1}{2}}\theta, \tag{2.11a,b}$$

where b is an arbitrary constant. Obviously we must have

$$\langle w\theta \rangle = \langle u_3 T^* \rangle / b^2 = F/b^2. \tag{2.11c}$$

Then (2.9 a) and (2. 11) combine to give

$$R = \frac{\langle |\nabla\theta|^2 \rangle}{\langle w\theta \rangle} + (RF)\frac{\langle (\overline{w\theta} - \langle w\theta \rangle)^2 \rangle}{\langle w\theta \rangle^2}, \tag{2.12a}$$

or equivalently

$$F = \frac{\langle w\theta \rangle^2 [1 - R^{-1}\langle |\nabla\theta|^2 \rangle / \langle w\theta \rangle]}{\langle (\overline{w\theta} - \langle w\theta \rangle)^2 \rangle}, \tag{2.12b}$$

where w and θ vanish at the boundary, have a zero horizontal mean, satisfy the scaling constraint (2.11 c) and satisfy

$$\nabla^2 w - \nabla_1^2 \theta = 0 \tag{2.12c}$$

in the layer. With $RF = \mu$, equation (2.12 a) will at once be recognized as the variational functional of BJ, and (2.12 b) obviously corresponds to Chan's functional for the fluid-layer case.

Next we define a class H of admissible functions:

$$H \equiv \{w, \theta: \nabla^2 w - \nabla_1^2 \theta = 0,\ w = \theta = 0|_{z=0,1},\ \overline{w} = \overline{\theta} = 0\}.$$

Among the elements $(w, \theta) \in H$ are those which also satisfy the scaling constraint $\mathcal{N}$:

$$\mathcal{N} \equiv \{w, \theta: \langle w\theta \rangle = F/b^2 = \mu/Rb^2\}.$$

Every statistically stationary solution is an element of $H \cap \mathcal{N}$.

We seek, therefore, to maximize F in (2.12 b) for all those elements in H which also satisfy the condition $\mathcal{N}$. However, since F is a homogeneous functional of degree zero, we can always renormalize the elements $(\tilde{w}, \tilde{\theta})$, which maximize F in H, so as to satisfy the condition $\mathcal{N}$. Thus we may obtain a unique element $(\hat{w}, \hat{\theta})$ in $H \cap \mathcal{N}$ which maximizes F. Hence our problem is reduced to finding the maximum of F in (2.12 b) for all elements in H.

Following Howard's arguments, it can be shown that maximizing F in (2.12b) for a given value of R is exactly equivalent to minimizing R in (2.12a) for a given value of μ ($= RF$). As a matter of fact, both problems lead to exactly the same Euler equations.

So far we have treated b as an arbitrarily re-assigned scalar quantity. In an alternative approach, however, we can first find an extremalizing element $(\tilde{w}, \tilde{\theta})$ in H, and then calculate b from (2.11c) so that the normalizing condition $\mathcal{N}$ is automatically satisfied.

3. Multi-α solutions

Using the method of Lagrange multipliers, extremalizing either (2.12a) or (2.12b) can be shown to lead to the same Euler equations:

$$\frac{1}{RF}\nabla^4\theta + \left(2+\frac{\lambda}{F}\right)\nabla^2 w - \frac{1}{\langle w\theta\rangle}[\nabla^2\{w\overline{w\theta}\} + \overline{w\theta}\nabla^2 w] = 0, \tag{3.1a}$$

$$\nabla^2 w - \nabla_1^2\theta = 0, \tag{3.1b}$$

$$w = \theta = \nabla^2\theta = 0 \quad \text{at} \quad z = 0, 1, \tag{3.1c}$$

where

$$\lambda = 2 - \frac{1}{R}\frac{\langle|\nabla\theta|^2\rangle}{\langle w\theta\rangle}. \tag{3.1d}$$

Here $\nabla^2\theta = 0$ arises as a natural boundary condition, and it can be shown that $1 \leqslant \lambda \leqslant 2$.

Equation (3.1a) is nonlinear, but the nonlinearity enters only through terms $\overline{w\theta}$ which depend on z alone. These equations therefore admit separable solutions of the form (Busse 1969)

$$w(x,y,z) = \sum_1^N w_n(z)\,\phi_n(x,y)$$

and

$$\theta(x,y,z) = \sum_1^N \theta_n(z)\,\phi_n(x,y), \tag{3.2a}$$

where $\phi_n(x,y)$ are eigenfunctions of the horizontal Laplacian

$$\nabla_1^2\phi_n = -\alpha_n^2\phi_n \tag{3.2b}$$

and

$$\overline{\phi_n\phi_m} = \delta_{mn}.$$

Since $\overline{w} = \overline{\theta} = 0$ we must have $\alpha_n^2 \neq 0$ for all n. Substituting (3.2) into (3.1), and writing

$$L_n w_n = (D^2 - \alpha_n^2)\,w_n = -\alpha_n^2\theta_n, \quad D \equiv d/dz, \tag{3.3}$$

we get

$$L_n^3 w_n = p\alpha_n^2 L_n w_n - q\alpha_n^2[L_n\{w_n\overline{w\theta}\} + \overline{w\theta}L_n w_n], \tag{3.4}$$

where

$$p = 2RF + R\lambda, \tag{3.5}$$

$$q = RF/\langle w\theta\rangle = \mu/\langle w\theta\rangle, \tag{3.6}$$

and

$$\langle w\theta\rangle = \langle\overline{w\theta}\rangle = \left\langle -\sum_1^N w_n\frac{L_n w_n}{\alpha_n^2}\right\rangle$$

$$= -\sum_1^N\left\langle\frac{w_n L_n w_n}{\alpha_n^2}\right\rangle. \tag{3.7}$$

The boundary conditions become

$$w_n = D^2 w_n = D^4 w_n = 0 \quad \text{at} \quad z = 0, 1. \tag{3.8}$$

To extremalize the functionals F or R in (2.12), we must also find the optimizing wavenumbers. For this we require that

$$\frac{dR}{d(1/\alpha_n^2)} = -\frac{1}{\alpha_n^4}\frac{dR}{d\alpha_n^2} = 0,$$

where we have noted that the variation of R which is associated with the change in w_n (call this $\delta_{\alpha_n^2} R$) vanishes whenever R is stationary. We find that

$$\left[\langle w\theta\rangle \partial_{\alpha_n^2}\left\langle \sum_1^N \left(1-\frac{D^2}{\alpha_n^2}\right) w_n \alpha_n^2 \left(1-\frac{D^2}{\alpha_n^2}\right)^2 w_n \right\rangle - \langle |\nabla\theta|^2\rangle \langle -w_n D^2 w_n\rangle\right] \Big/ \langle w\theta\rangle^2$$
$$+ RF[\langle w\theta\rangle^2 \partial_{\alpha_n^2}\langle \overline{w\theta}^2\rangle - 2\langle \overline{w\theta}^2\rangle \langle w\theta\rangle \langle -w_n D^2 w_n\rangle]/\langle w\theta\rangle^4 = 0, \tag{3.9}$$

where

$$\partial_{\alpha_n^2}\left\langle \sum_1^N \left(1-\frac{D^2}{\alpha_n^2}\right) w_n \alpha_n^2 \left(1-\frac{D^2}{\alpha_n^2}\right)^2 w_n \right\rangle = \left\langle (-D^2 w_n)\alpha_n^2 \left(1-\frac{D^2}{\alpha_n^2}\right)^2 w_n \right\rangle$$
$$- \left\langle \left(1-\frac{D^2}{\alpha_n^2}\right) w_n \alpha_n^4 \left(1-\frac{D^2}{\alpha_n^2}\right)^2 w_n \right\rangle + \left\langle \left(1-\frac{D^2}{\alpha_n^2}\right) w_n \alpha_n^2 \left(-2D^2 + 2\frac{D^4}{\alpha_n^2}\right) w_n \right\rangle$$

and

$$\partial_{\alpha_n^2}\langle \overline{w\theta}^2\rangle = \partial_{\alpha_n^2}\left\langle \left\{ \sum_1^N w_n \left(1-\frac{D^2}{\alpha_n^2}\right) w_n \right\}^2 \right\rangle$$
$$= \left\langle -2\left\{ \sum_1^N w_n \left(1-\frac{D^2}{\alpha_n^2}\right) w_n \right\} w_n D^2 w_n \right\rangle.$$

We are required, therefore, to solve (3.4) subject to the boundary conditions (3.8) and the wavenumber optimizing equations (3.9).

A few comments are in order here regarding the role of the parameters p and q in (3.4)–(3.6). It is at once apparent that, if $(\{w_n\}, \{\alpha_n^2\}; q)$ is a solution of (3.4) for a given value of p, so is $(a\{w_n\}, \{\alpha_n^2\}; q/a^2)$, where a is an arbitrary scaling parameter. Thus, fixing q fixes the size of the solution $\{w_n\}$, and this size plays the role of an 'eigenvalue' of the nonlinear two-point boundary-value problem (3.4) with (3.8). Thus p is the independent parameter in this problem. For a given value of p, we can choose any value of q, and solve (3.4) and (3.8), optimizing α_n^2 using (3.9). Having obtained the solution $(\{w_n\}, \{\alpha_n^2\}; q)$, $\mu = RF$ may be calculated from (3.6). Then R may be calculated from (2.12a) and, hence, $F = \mu/R$ and $Nu = 1 + F$. Thus, fixing p determines every other quantity of the problem.

The solutions of (3.3), (3.4) and (3.8) are characterized by the following orthogonality relation:

$$(\alpha_l^2 - \alpha_n^2)\left[\frac{(\alpha_l^2-\alpha_n^2)^2}{\alpha_l^2\alpha_n^2}\langle Dw_l Dw_n\rangle - \langle \alpha_l^2 + \alpha_n^2\rangle\langle \theta_l\theta_n\rangle \right.$$
$$\left. - \langle D\theta_l D\theta_n\rangle + p\langle w_n w_l\rangle - 2q\langle \overline{w\theta} w_n w_l\rangle\right] = 0. \tag{3.10}$$

To derive (3.10) we first note that (3.8) and (3.3) show that $\theta_n = D^2\theta_n = L_n\theta_n = 0$ at $z = 0, 1$. Then we form the relation

$$\langle w_l\,[\text{equation (3.4)}]\rangle - \langle w_n\,[\text{equation (3.4) with } n \text{ replaced by } l]\rangle = 0. \tag{3.11}$$

After repeated integration by parts, using (3.3) and the boundary conditions, we find that

$$\frac{-\langle w_l L_n^3 w_n\rangle}{\alpha_n^2} = \langle w_l L_n^2 \theta_n\rangle$$
$$= \frac{(\alpha_l^2-\alpha_n^2)}{\alpha_n^2}\langle Dw_l Dw_n\rangle + (\alpha_l^2-\alpha_n^2)^2\langle w_l w_n\rangle - \alpha_l^2(\alpha_l^2-\alpha_n^2)\langle\theta_l\theta_n\rangle$$
$$+\alpha_l^2\langle D\theta_l D\theta_n\rangle + \alpha_l^2\alpha_n^2\langle\theta_l\theta_n\rangle, \tag{3.12a}$$

$$\langle w_l L_n w_n\rangle = -\langle Dw_n Dw_l\rangle - \alpha_n^2\langle w_l w_n\rangle \tag{3.12b}$$

and
$$\langle w_l L_n(w_n\overline{w\theta}) + w_l\overline{w\theta}L_n\theta_n\rangle$$
$$= (\alpha_l^2-\alpha_n^2)\langle w_n w_l\overline{w\theta}\rangle - \langle\overline{w\theta}(\alpha_l^2\theta_l w_n + \alpha_n^2\theta_n w_l)\rangle. \tag{3.12c}$$

The orthogonality condition (3.10) follows from (3.11) using (3.12*a*, *b*, *c*).

The conditions (3.10) appear to have some features close to orthogonality conditions which are familiar from linear eigenvalue problems. In particular, it is possible that (3.10) is associated with the fact that 'eigensolutions' of (3.4) belonging to α_i have nodal separation properties. Consistent with (3.10) we assumed that, when two-α solutions exist, the 'eigenfunction' belonging to α_1 is an even function and the 'eigenfunction' belonging to α_2 is an odd function. We then found numerically α_1 eigenfunctions that had no nodes and the α_2 eigenfunctions that had one node at $z = \frac{1}{2}$.

The conditions (3.10) differ from familiar orthogonality conditions in that (3.10) depend explicitly on the 'eigenvalues' α_i as well as on the 'eigenfunctions'. In addition, for each finite R (or p) there is only a finite number $N < \infty$ of 'eigenfunctions'.

4. Heat transport when R is near R_c.

It is well known and easily shown that

$$\min_H\left\{\frac{\langle|\nabla\theta|^2\rangle}{\langle w\theta\rangle}\right\} = \min_{\alpha_n, w_n}\frac{\sum_1^\infty\left\langle\alpha_n^2\left(1-\frac{D^2}{\alpha_n^2}\right)w_n\left(1-\frac{D^2}{\alpha_n^2}\right)^2 w_n\right\rangle}{\sum_1^\infty\left\langle w_n\left(1-\frac{D^2}{\alpha_n^2}\right)w_n\right\rangle}$$
$$= \min_{\alpha_1, w_1}\frac{\left\langle\alpha_1^2\left(1-\frac{D^2}{\alpha_1^2}\right)w_1\left(1-\frac{D^2}{\alpha_1^2}\right)^2 w_1\right\rangle}{\left\langle w_1\left(1-\frac{D^2}{\alpha_1^2}\right)w_1\right\rangle} = 4\pi^2,$$

the minimum being obtained for

$$w_1(z) = \sin\pi z, \quad \alpha_1^2 = \pi^2, \quad \theta_1(z) = (1-D^2/\alpha_1^2)w_1 = 2\sin\pi z. \tag{4.1}$$

Hence, whenever $R < 4\pi^2$, F in (2.12*b*) will be negative for any non-zero (w, θ), b from (2.11*c*) will be imaginary, and hence (u_3, T^*) from (2.11*a*, *b*) will also be imaginary. Thus we must have $u_3 = T^* = 0 = F$, and statistically stationary convection with $R < 4\pi^2$ is not possible. On the other hand, it is known from the linear theory of stability that steady convection commences when $R > 4\pi^2$.

Hence, $4\pi^2$ is a global limit of stability for the conduction solution of the DOB equation (Westbrook 1969). We note that, as $R \downarrow 4\pi^2$, $b \to 0$. Hence the single-α solution appears first with an infinitesimal magnitude as a bifurcation of the zero solution at the point of bifurcation $R = p = 4\pi^2$.

We may also compute the slope of the heat-transport curve at $R = 4\pi^2$ or $\mu = 0$. For any $\mu \geqslant 0$, from (2.12a) we get

$$\frac{dR}{d\mu} = \frac{\partial R}{\partial \mu}\bigg|_{w,\,\theta} + \frac{\delta R}{\delta \mu}\bigg|_{\mu} = \frac{\partial R}{\partial \mu} = \frac{\langle (\overline{w\theta} - \langle w\theta \rangle)^2 \rangle}{\langle w\theta \rangle^2}, \tag{4.2}$$

where $\delta R/\delta\mu$ gives the variation of

$$R(\mu) = R(\tilde{w}(\mu), \tilde{\theta}(\mu); \mu)$$

with w and θ when the third place variable μ is fixed. Since R is stationary with respect to variations in w and θ, and since $\partial\tilde{w}/\partial\mu$ and $\partial\tilde{\theta}/\partial\mu$ belong to H, $\delta R/\delta\mu = 0$. At $\mu = 0$ using (4.1) and (4.2) we get

$$\frac{dR}{d\mu}\bigg|_{\mu=0} = \frac{dR}{d(RF)}\bigg|_{RF=0} = \frac{1}{2} \quad \text{or} \quad R\frac{dF}{dR} = 2 \quad \text{or} \quad \frac{dNu}{dR} = \frac{1}{2\pi^2}. \tag{4.3}$$

It was shown in BJ that there exists an exact solution of the DOB equations with $B = 0$ such that

$$[dNu/dR]_{R=4\pi^2} = 1/2\pi^2.$$

Hence, the bounding heat-transport curve coincides with an exact solution in the immediate neighbourhood of $R = 4\pi^2$.

We have seen that the maximizing solution (4.1) for F has a single horizontal mode at $R = p = 4\pi^2$. It is quite reasonable to assume that for a certain range $4\pi^2 \leqslant R \leqslant R_{12}$, or equivalently $4\pi^2 \leqslant p \leqslant p_{12}$, the extremalizing solution will still be characterized by one single horizontal mode. At $R = R_{12}$ (or $p = p_{12}$), the single-α solution would bifurcate into a two-α solution. This assumption is completely consistent with theory as it is presently understood, and is supported by the numerical analysis of BJ and this investigation. In general, one expects repeated bifurcation of solutions with N wavenumbers to solutions with $N+1$ wavenumbers as R (or p) is increased.

In the next section we shall solve the single-α problem associated with (3.4) numerically for $p > 4\pi^2$.

5. Numerical computation of the single-α solution

With $N = 1$, equations (3.4) and (3.8) define a sixth-order nonlinear differential equation with two-point boundary conditions. As indicated earlier in § 3, for a given value of $p > 4\pi^2$ we can assign any value to q (thus fixing the 'size' of the solution w_1) and make a guess for the optimum value of α_1^2. Knowing p, q and α_1^2, we may solve the sixth-order two-point boundary-value problem by the well-known shooting method. In general, however, the initially guessed value of α_1^2 will not satisfy the wavenumber optimizing equation (3.9). To find a better value of α_1^2, we use the computed solution w_1 in (3.9) to form a polynomial (with known

coefficients) in the variable α_1^2. This polynomial is then solved for a new value of α_1^2. Differential equation (3.4) is then solved again using this new value of α_1^2, and the old values of p and q. This process is repeated again and again until the difference between two successive iterates of α_1^2 is tolerably small. Finally, knowing the solution (w_1, α_1^2, q), $\mu = RF$ may be calculated from (3.6). Then R may be calculated from (2.12a), and the values $F = \mu/R$ and $Nu = 1+F$ follow immediately.

To keep the number of α_1^2-iterations small, it is very important to estimate a starting value of α_1^2 close to its optimizing value. For this purpose, results for the two lower values of p are extrapolated linearly to the new value of p on a log–log scale. To further speed up the convergence of α_1^2-iterates, Aitken's extrapolation procedure is used after every two α_1^2-iterations.

The numerical integration in the shooting method was performed using a Runge–Kutta method with a variable step size. The step size is repeatedly halved by the subroutine until a specified relative accuracy (10^{-5}) in results is obtained.

The numerical computation of the solution w_1 was facilitated by assuming that w_1 is an even function of $z-\frac{1}{2}$ for $0 \leqslant z \leqslant 1$. This is suggested by the symmetry of equations (3.4), (3.8) and (4.1) about $z = \frac{1}{2}$. This symmetry assumption implies that

$$Dw_1 = D^3w_1 = D^5w_1 = 0 \quad \text{at} \quad z = \tfrac{1}{2}.$$

The whole problem can thus be solved in a half layer, reducing the required computer time by approximately one half. It was also found that the numerical integration of the problem is easier and more accurate when integrating from $z = 0{\cdot}5$ to $z = 1{\cdot}0$ (i.e. from centre of the channel to the boundary) rather than from $z = 0$ to $z = 0{\cdot}5$. The explanation probably lies in the fact that the solution w_1 is better behaved at the centre than at the boundary.

The shooting method worked quite well for low values of p. However, for $p > 300$ the integration becomes quite sensitive to the initial condition; i.e. even a slight inaccuracy in the assumed initial conditions causes divergence in the process of their correction or causes the initial-value problem to become unbounded before the integration can be carried through to the other end.

To circumvent the difficulty encountered with the shooting method, the Newton–Kantorovitch or quasi-linearization technique (Bellman & Kalaba 1965) was tried. This method gives good results for all values of p but becomes prohibitively expensive at large values of p. The basic idea behind the technique is to 'linearize' the original nonlinear problem about a certain trial function, and then to 'iterate' on this linear problem until two consecutive iterates are essentially the same and hence equal to the solution of the original nonlinear problem. For example, equation (3.4) for the single-α case may be written symbolically as

$$D^6w_1 = f(w_1, Dw_1, D^2w_1, D^3w_1, D^4w_1, D^5w_1).$$

We can linearize this equation as follows:

$$D^6w_1 = (f)_0 + (\partial f/\partial w_1)_0\{w_1 - (w_1)_0\} + (\partial f/\partial(Dw_1))_0\{Dw_1 - (Dw_1)_0\} + \ldots + (\partial f/\partial(D^5w_1))_0\{D^5w_1 - (D^5w_1)_0\},$$

where the subscript zero denotes the value of the expression inside the parentheses evaluated for some initial function $(w_1)_0$. Thus, for example, a term like w_1^3 on the right-hand side of (3.4) would be linearized as

$$w_1^3 = (3w_1^2)_0\{w_1 - (w_1)_0\} + (w_1^3)_0 = 3(w_1)_0^2\{w_1 - (w_1)_0\} + (w_1^3)_0.$$

Of course this scheme leaves the linear terms unchanged. The idea behind linearization is that a linear boundary-value problem can be solved easily by the superposition of its linearly independent solutions in such a way that all boundary conditions are satisfied, while there is no such procedure for a nonlinear equation.

Even though, theoretically, a linear differential equation can be solved by properly combining its linearly independent solutions, the procedure leads to completely incorrect results when applied as a numerical technique on high-speed computers with only limited accuracy. The basic problem is that one eigenfunction of the differential operator grows much more rapidly than the others as the independent variable goes from one end to the other. As a result, regardless of their initial behaviour, all solutions of the equation become dependent on only the most rapidly growing eigenfunction and essentially independent of the slower growing ones. The problem and its solution are described in detail by Conte (1966). Essentially the remedy lies in ortho-normalizing the independent solution-vectors as soon as any two of them become nearly parallel. No more need be said about this except that the ortho-normalizing matrix seems to have been printed wrongly in Conte's paper. Its elements p_{ij} should be as follows:

$$p_{ij} = \begin{cases} \sum_{k=i}^{j-1} -(z^k, y^j)\, p_{ik}/w_{jj} & (i < j), \\ 0 & (i > j), \\ 1/w_{ii} & (i = j). \end{cases}$$

Conte's technique was found to work very well for our problem.

In using the quasi-linear method of Newton–Kantorovitch, we must select a proper function as a first iterate. The solution w_1 for a lower value of p is an appropriate choice for this purpose. However, we do not have to store the whole function into the computer memory. Instead we can regenerate this solution again and again as it is needed in the integration, provided we know the correct corresponding values of p, q and α_1^2 and w_1, D^2w_1 and D^4w_1 at $z = \frac{1}{2}$.

Similarly, it is also convenient to keep regenerating the successive iterates of w_1 in the Newton–Kantorovitch scheme as and when they are needed instead of storing them. This requires more computer time but less storage. More important, however, this method is more accurate and reliable.

The computer programs used in these computations are listed in Gupta's (1972) thesis. The results are given in table 1, which lists the corresponding values of p, q, α_1^2, $w_1(\frac{1}{2})$, $D^2w_1(\frac{1}{2})$, $D^4w_1(\frac{1}{2})$, R and F. The solution $w_1(z)$ and q have been renormalized here in such a way that $\langle w\theta\rangle = \langle w_1\theta_1\rangle = 1$. This was done to keep some comparability between solutions belonging to different values of p. Note that in this case $\mu = RF = q$.

In the next section we consider the two-α problem and the associated bifurcation problem.

p/R	$q\ (=\mu)/F$	α_1^2	$w_1(\frac{1}{2})$	$D^2w_1(\frac{1}{2})$	$D^4w_1(\frac{1}{2})$
39·47841760	0·0	9·869604401	1·0	−9·869604401	97·40909103
39·47841760	0·0	—	—	—	—
100·0	20·878814872	10·054427750	0·99255669288	−8.891838926	12·337596275
49·18557724	0·4244905935	—	—	—	—
200·0	57·346027010	10·894366176	0·99399315060	−7·701654079	−82·381978702
63·67971483	0·9083901704	—	—	—	—
300·0	96·961614503	12·033709850	1·0008563972	−6·802244467	−140·81112198
76·54062831	1·266799302	—	—	—	—
500·0	179·01345478	14·466012415	1·0137460926	−5·539809288	−192·79428548
98·66969450	1·814269880	—	—	—	—
750·0	285·54560674	17·320966008	1·0239518708	−4·565352893	−204·35134029
121·9495495	2·341506040	—	—	—	—
1000·0	394·59169805	19·926778779	1·0301043655	−3·935745154	−199·62187657
142·2027274	2·774853234	—	—	—	—
1500·0	617·14107958	24·590584521	1·0366244674	−3·140972601	−185·38867797
177·1649796	3·483425906	—	—	—	—
2000·0	843·41616087	28·746376527	1·0395347384	−2·632170779	−174·27566624
207·4311736	4·066004864	—	—	—	—
2250·0	957·52067541	30·694683255	1·0403260346	−2·434617306	−169·69031834
221·3422105	4·325974125	—	—	—	—
2256·2	960·35715800	30·741746408	1·0403411286	−2·430099349	−169·58238429
221·6785859	4·332205359	—	—	—	—
2262·5	963·23970333	30·789509965	1·0403562704	−2·425525724	−169·47296719
222·0199834	4·338527048	—	—	—	—
2275·0	968·95996884	30·884104745	1·0403857367	−2·416501972	−169·25663154
222·6961617	4·351040275	—	—	—	—
2300·0	980·40417414	31·072605842	1·0404424173	−2·398654550	−168·82694772
224·0437839	4·375949009	—	—	—	—
2350·0	1003·3070204	31·446904099	1·0405471469	−2·363737051	−167·97913027
226·7204270	4·425304918	—	—	—	—
2400·0	1026·2286305	31·817688810	1·0406410462	−2·329814369	−167·14598796
229·3728892	4·474062450	—	—	—	—
2500·0	1072·1259537	32·549133065	1·0407993108	−2·264768946	−165·52051789
234·6080840	4·569859381	—	—	—	—
2750·0	1187·1631345	34·326535653	1·0410563469	−2·116402130	−161·66116365
247·3188892	4·800131274	—	—	—	—
3000·0	1302·5895596	36·073503057	1·0412029429	−1·983027383	−158·01258614
259·5464347	5·018714903	—	—	—	—
3250·0	1418·3482598	37·758964118	1·0412234433	−1·864285408	−154·54511000
271·3458647	5·227086329	—	—	—	—
3500·0	1534·4038868	39·391241805	1·0411531419	−1·757669345	−151·22745834
282·7634663	5·426457338	—	—	—	—
3600·0	1580·9007346	40·025529133	1·0411007620	−1·718257260	−149·94263076
287·2322475	5·503911028	—	—	—	—
3750·0	1650·7222293	40·962832376	1·0410051277	−1·661996345	−148·05297673
293·8371845	5·617812573	—	—	—	—
4000·0	1767·2977968	42·535567403	1·0408415175	−1·572854516	−144·94304341
304·6010670	5·802007899	—	—	—	—
6000·0	2706·5364652	53·807628490	1·0386195404	−1·077729476	−123·38142754
382·1326256	7·082714963	—	—	—	—
8000·0	3662·2447481	63·587200493	1·035017418	−0·791276781	−106·1273086
449·0118706	8·138192430	—	—	—	—

TABLE 1. Values of the parameters for the single-α solution

6. Numerical computation of the two-α solution

When $N = 2$ we get two Euler differential equations from (3.4) with $n = 1$ and $n = 2$. We shall denote the corresponding solutions by $w_1^{[2]}(z,p)$ and $w_2^{[2]}(z,p)$. The superscripts have been added to differentiate this solution from the single-α solution. However, we simplify the notation by suppressing the superscripts where the context makes it clear.

The two-α problem is governed by a twelfth-order differential equation system instead of the sixth-order system which governs the single-α case. We shall assume again that $w_1^{[2]}$ is an even function of $z-\frac{1}{2}$, and that $w_2^{[2]}$ is an odd function. These symmetry properties prevail in the problem treated by BJ, and they reduce the orthogonality condition (3.10) to an identity. These assumptions imply that

$$\left.\begin{aligned} Dw_1 = D^3w_1 = D^5w_1 = 0 \quad &\text{at} \quad z = \tfrac{1}{2}, \\ w_2 = D^2w_2 = D^4w_2 = 0 \quad &\text{at} \quad z = \tfrac{1}{2}, \\ w_i = D^2w_i = D^4w_i = 0 \quad &\text{at} \quad z = 1 \quad \text{for} \quad i = 1, 2. \end{aligned}\right\} \tag{6.1}$$

We can treat this two-α problem using the Newton–Kantorovich scheme (with Conte's ortho-normalizations) in exactly the same way as in the single-α problem. In the latter case, however, we knew the analytical solution (4.1) for $p = 4\pi^2$, which we were able to use as a first iterate in the computation of the single-α solution at a higher value of p. The corresponding information in the two-α case can be obtained from our assumption that at a critical value $p = p_{12}$ the single-α solution bifurcates into a two-α solution. When p is above p_{12} but close to it, the second mode $w_2^{[2]}$ is expected to be small compared with the first mode. Hence $w_2\theta_2$ may be neglected in comparison with $w_1\theta_1$. Equation (3.4) with $n = 1$ then reduces to the Euler equation for the single-α case, whose solution we already know. Equation (3.4) for the second mode, however, reduces to

$$L_2^3 w_2 = \alpha_2^2 p L_2 w_2 - q\alpha_2^2[L_2(w_1\theta_1 w_2) + w_1\theta_1 L_2 w_2], \tag{6.2}$$

subject to the boundary conditions (6.1). This defines a linear eigenvalue problem for w_2 with eigenvalue $\Lambda = \alpha_2^2$. Knowing $p > p_{12}$, q and the corresponding w_1, we may solve this eigenvalue problem for a non-trivial solution w_2 and the eigenvalue Λ. No such solution is expected to exist for $p < p_{12}$. The results of this linear eigenvalue problem are listed in table 2. It is at once clear that p_{12} lies between 2250 and 2265. Corresponding values of R from the single-α solution are 221·34 and 222·02. More accurate information about the bifurcation point can be obtained from backward extrapolation of the two-α results obtained later. This extrapolation gives

$$p_{12} \cong 2252{\cdot}5, \quad R_{12} \cong 221{\cdot}5, \quad \Lambda = \alpha_2^2 \cong 111{\cdot}7$$

at the point of bifurcation.

The solution w_2 of the linear eigenvalue problem (for $p = 2262{\cdot}5$) is shown in figure 1. Note that no scale is shown on the y axis since w_2 is the solution of a homogeneous linear problem.

p	Λ
3500·0	76·112
3250·0	76·550
3000·0	77·628
2750·0	79·862
2500·0	85·053
2250·0	No solution
2400·0	89·141
2350·0	92·284
2300·0	97·189
2275·0	101·393
2262·5	104·995

TABLE 2. Variation of the eigenvalue parameters for the eigenvalue problem (6.2) for the point of bifurcation of the single-α solution

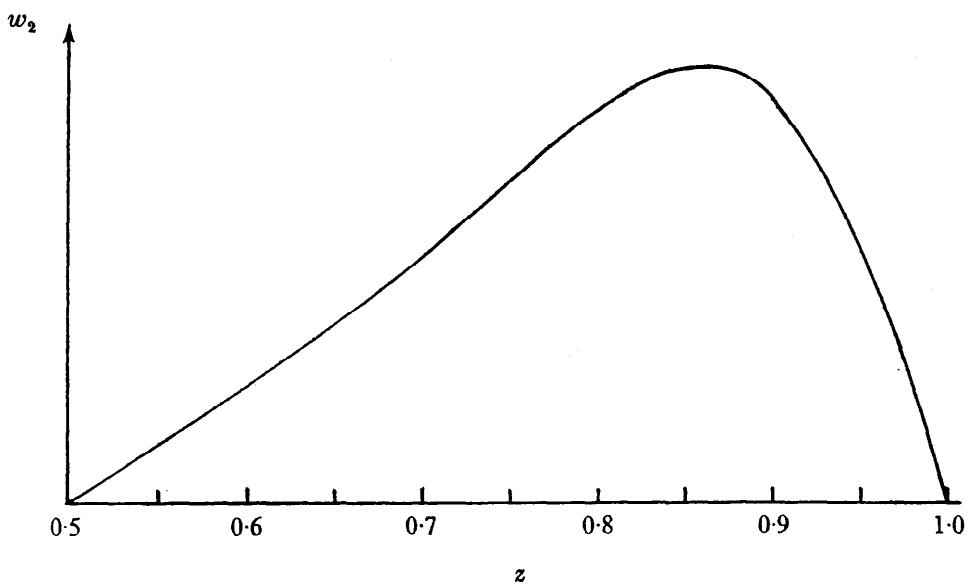

FIGURE 1. The second-mode eigenfunction at the point of bifurcation, $p = p_{12}$.

Results of this linear eigenvalue problem can now be used in the solution of the two-α problem. For a value of p close to p_{12}, we can use (as the first iterates in the Newton–Kantorovich scheme) the single-α solution for the first mode and the solution of (6.2) for the second mode. The first iterate of the second mode must, however, be 'suitably' scaled. If we scale it too small, the Newton–Kantorovich scheme makes the second mode converge to zero and the first mode converge to the single-α solution. This combination is always a solution to the governing equations. On the other hand, if we scale it too large, the Newton–Kantorovitch scheme converges to the correct two-α solution but very slowly. The suitable scaling range is found by trial and error.

Once, however, the correct two-α solution is known for a particular value of p (say 2265) this solution can be used as a first iterate for a higher value of p, provided, of course, that the difference between the two values of p is not too large. Thus we can construct the whole two-α solution for any desired range of p. As in

$\frac{p}{R}$	$q/(F = Nu-1)$	$\frac{\alpha_1^2}{\alpha_2^2}$	$\frac{w_1(\frac{1}{2})}{Dw_2(\frac{1}{2})}$	$\frac{D^2w_1(\frac{1}{2})}{D^3w_1(\frac{1}{2})}$	$\frac{D^4w_1(\frac{1}{2})}{D^5w_1(\frac{1}{2})}$
2265·0	964·46784585	30·501313092	1·0390844210	−2·483129703	−170·05641634
222·1647457	4·341228141	111·82578231	0·18338160417	5·1259590055	−238·82244201
2282·5	972·60289889	30·212534479	1·0373267924	−2·553231984	−170·61165572
223·1225654	4·359052152	111·96693667	0·28452569235	7·9774400581	−375·30264212
2300·0	980·74008941	29·923520099	1·0355604516	−2·622450990	−171·12564396
224·0749411	4·376839663	112·10899682	0·35694833314	10·038947066	−476·81928363
2325·0	992·36147131	29·554176294	1·0331979058	−2·712363379	−171·74132448
225·4254949	4·402170533	112·36290984	0·43399577140	12·270803658	−588·96436759
2350·0	1003·9852958	29·196455622	1·0308723887	−2·798626993	−172·27866236
226·7653565	4·427419211	112·61435690	0·49660073111	14·114163550	−684·28285811
2400·0	1027·2370986	28·536321615	1·0264273933	−2·957111599	−173·13448727
229·4139867	4·477656805	113·16015395	0·59456373047	17·086955146	−842·28168094
2500·0	1073·7626927	27·399330385	1·0182816132	−3·226999519	−174·22463104
234·5958494	4·577074555	114·38891755	0·73094257083	21·523157712	−1084·5799567
2600·0	1120·3241882	26·454278378	1·0110065361	−3·447063776	−174·80888809
239·6381727	4·675065645	115·76230080	0·82404670606	24·914725854	−1268·7144504
2750·0	1190·2430899	25·302140950	1·0014663481	−3·707724235	−175·22759778
246·9700227	4·819382843	118·01939079	0·91882195028	28·978139504	−1475·6711277
3000·0	1306·9899059	23·878627150	0·98853173636	−4·013261058	−175·55364482
258·6576269	5·052972617	122·13773970	1·0097875531	34·284488799	−1695·3548808
3500·0	1541·2861835	22·066281735	0·97016325656	−4·353226392	−176·4540582
280·4332149	5·496089984	131·26354461	1·0716548027	42·322355212	−1831·0096582
4000·0	1776·5356007	20·999115599	0·95818482380	−4·509549675	−177·85006864
300·5483475	5·910981097	140·82009387	1·0632327285	48·396482556	−1706·2835227
4500·0	2012·6078857	20·344480854	0·95028441144	−4·572500069	−179·48796931
319·3678432	6·301848881	150·75679800	1·0220546340	53·141851611	−1393·1760262
5000·0	2249·3871456	19·934284453	0·94501362865	−4·585799593	−181·01567968
337·1314852	6·672136079	160·89359964	0·96586342949	56·777861239	−949·63922892
5500·0	2486·7822474	19·695045404	0·94163305358	−4·568894646	−182·33362119
354·0094259	7·024621566	171·24425401	0·90228782413	59·439363190	−411·20590671
6000·0	2724·7164690	19·542317355	0·93932775379	−4·537932510	−183·23393184
370·1284237	7·361543438	181·65563346	0·83752850944	61·266756403	178·32130156
7000·0	3201·9474209	19·450410967	0·93708969928	−4·453043056	−184·1422461
400·4596743	7·995680031	202·36368214	0·71428953055	62·816869103	1398·39473371
8000·0	3680·7162305	19·531542024	0·93676393680	−4·354999472	−184·12986213
428·6971667	8·585818887	223·15601452	0·60336883235	62·235748310	2576·60044112

TABLE 3. Values of the parameters for the two-α solution

the single-α case, we do not store any solutions into the computer memory. It is more convenient, reliable and accurate to regenerate any required solution from its known initial values.

The various two-α results are listed in table 3. Here, as in the single-α case, the results have been renormalized such that $\langle w\theta \rangle = \langle w_1\theta_1 + w_2\theta_2 \rangle = 1$. The computer programs used in these computations are listed in Gupta's thesis.

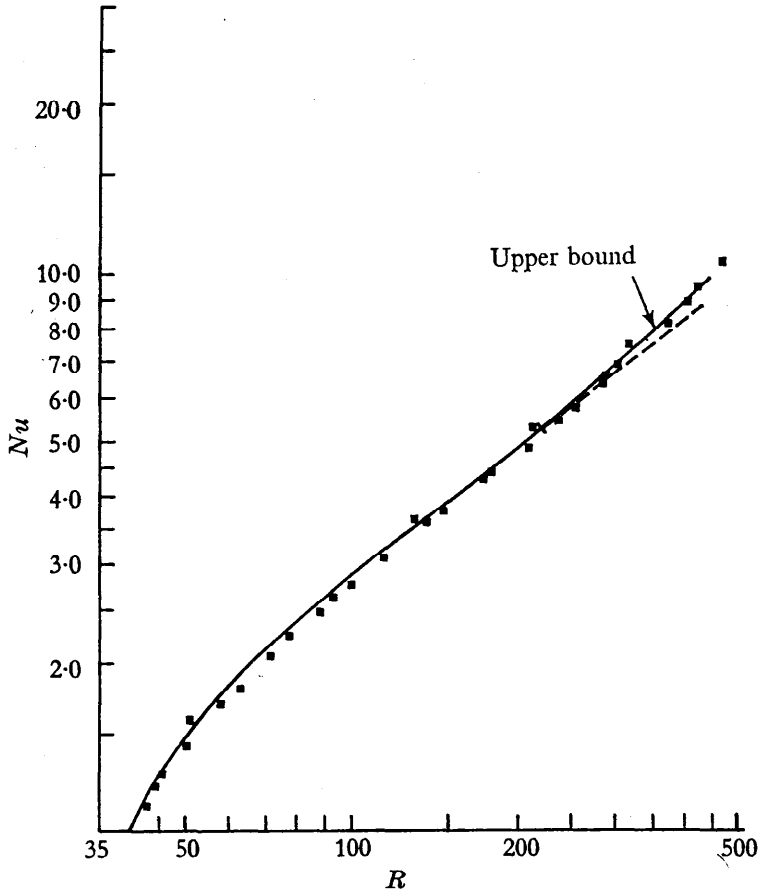

FIGURE 2. Comparison of the numerically computed bounding heat-transport curve with the experiments of Buretta & Berman (1973). – –, continuation of the single-α solution past the point of bifurcation.

7. The heat-transport curve: comparison of theory and experiment

A very well established feature of thermal convection in a pure fluid layer which was discovered by Malkus (1954*a*) is that the heat flux $Nu(R)$ varies in linear segments with R. It is natural to identify the points of transition between the 'straight line' segments as points where the nature of convection changes. Krishnamurti (1970*a*, *b*) has carefully examined this transition phenomenon anew and essentially confirmed and extended the earlier observations. She finds that the flow changes from steady two-dimensional rolls to another steady cellular motion as the first point of bifurcation is passed.

A similar transition phenomenon has been observed for convection in a porous layer by Combarnous & LeFur (1969) and by Buretta & Berman (1973). In the experiments of Buretta & Berman, heat-transfer measurements are obtained from different porous layers made up of packed glass beads (with 3, 6 and 14·3 mm diameters) in a cylindrical container of small aspect ratio (height/diameter ranges from $\frac{1}{10}$ to $\frac{1}{4}$).

In figure 2 we have compared all the measurements of the heat transport in Buretta & Berman's experiments in four out of five runs† with the theoretical

† The data from one run differed from the other four by about 10%. We do not know whether the inconsistent data is real or spurious.

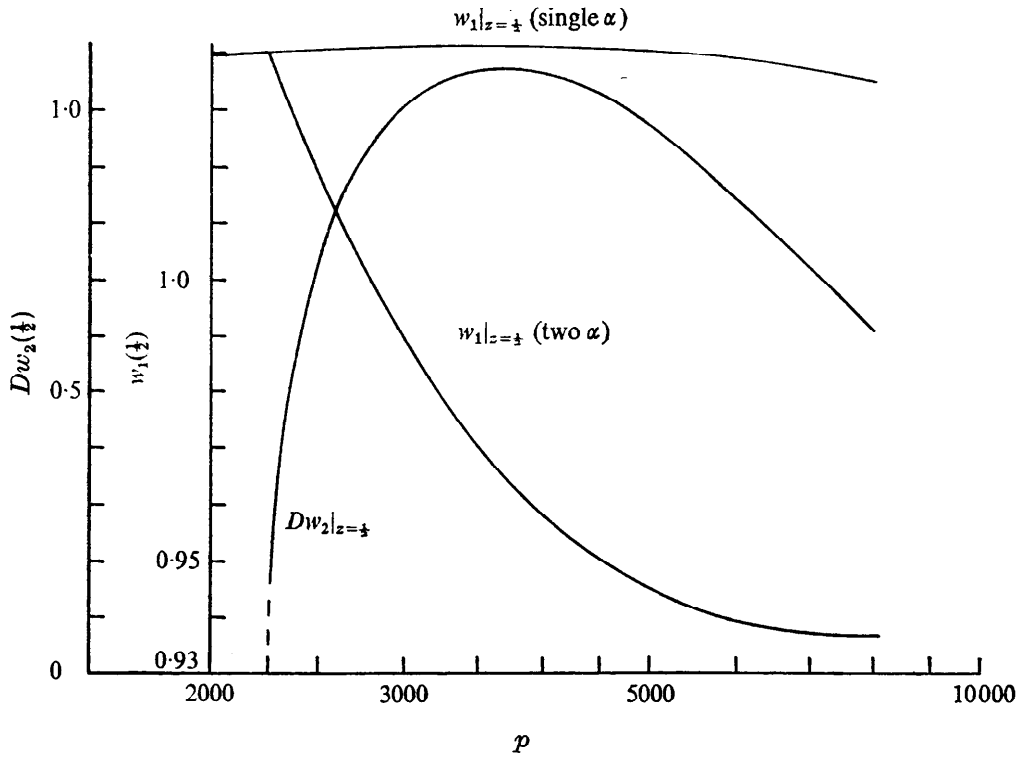

FIGURE 3. The variation of representative initial values for the two-α solution. This graph also gives a measure of the amplitude of the second mode which comes in at $p = p_{12}$ as a bifurcation with zero amplitude. Note the sharp change in slopes of these graphs as we go from the single-α solution to two-α solution. – –, extrapolation; ——, continuation of the single-α solution past the point of bifurcation.

upper bound calculated numerically. The agreement between the experiments and theory is striking. The data of Combarnous & LeFur also seems to be in good agreement with the theory but the published experimental data are plotted on such a small scale as to make detailed comparison with theory very difficult.

The nature of the agreement between theory and experiment with regard to the point of bifurcation is of particular interest. In making this comparison the continuity properties of the theoretical heat transport become important. We have noted already in (4.2) that

$$\frac{dR}{d\mu} = \frac{\langle(\overline{w\theta} - \langle w\theta\rangle)^2\rangle}{\langle w\theta\rangle^2} = \frac{\langle(w_1\theta_1 + w_2\theta_2 - \langle w_1\theta_1 + w_2\theta_2\rangle)^2\rangle}{\langle w_1\theta_1 + w_2\theta_2\rangle^2}. \tag{7.1}$$

The slope of the heat-transport curve is directly related to this quantity. At the point of bifurcation (where $w_2 = \theta_2 = 0$) it is obviously equal to its value for the single-α case. $d^2R/d\mu^2$ will obviously depend on $dw_1(z)/d\mu$ and $dw_2(z)/d\mu$. Figure 3, however, clearly shows that these quantities abruptly change when we go from the single-α solution to the two-α solution at the point of bifurcation. Hence, there is expected to be a jump in the second derivative (or curvature) of the bounding heat-transport curve at the point of bifurcation. This is not inconsistent with our numerical results.

Returning now to the experiments, we note that the observed changes in the slope of the heat-transport curve are not of sufficient precision to establish the nature of the discontinuity at the point of bifurcation. Indeed, transitions associated with secondary bifurcations may, in some cases, have the same continuity properties as the bounding heat-transport curve. There are, of course, instabilities of a 'snap through' type such as is observed in the breakdown of laminar pipe flow (cf. Joseph & Sattinger 1972). Such instabilities are usually associated with hysteresis phenomena and they would ordinarily lead to actual discontinuities in the heat-transport curve rather than to discontinuities in slope.

It follows, assuming the continuity of slope in the experiments, that the bifurcation would go undetected for some range of $R > R_{12}$ and the experimentally observed transition value would be too high. In view of this the values of 280–300 of Combarnous & LeFur and the value of 245 of Buretta are in good agreement with our numerically calculated value $R_{12} = 221{\cdot}5$.

After having made this case for agreement between theory and experiment, we must note that we have been selective in the data displayed in figure 2. In figure 8 we have plotted all of the data from three different papers available to us. There is considerable uncertainty in this data even when the experiments are carefully performed, and no experiment is guaranteed to have an error of less than 10%. It is therefore possible that points lying above the two-α numerical upper bound in figure 8 represent spurious observations.

We turn next to comparison of theory and experiment when R is large.

8. Asymptotic results for large R

A well-known dimensional argument which leads to the law $Nu \propto R^{\frac{1}{2}}$ as $R \to \infty$ in the case of regular convection leads to $Nu \propto R$ as $R \to \infty$ in the case of porous convection. An infinite limiting Rayleigh number can obviously be achieved by making d, the plate separation, tend to infinity while $\Delta T = T_2 - T_1$ is kept fixed. However, in this case the heat flux $(K\Delta T/d)\,Nu$ must be independent of d, being the heat flux into a semi-infinite region through a lower heated surface. Therefore, the Nusselt number must vary linearly with d. But the Nusselt number depends on d only through the Rayleigh number, which also varies linearly with d. Therefore, Nu must vary linearly with R as $R \to \infty$.

The argument just given depends, of course, upon the assumption that Nu depends on d only through R and not on other parameters which also depend on d. This would be true if the DOB equations were valid in the limit of large R. However, we cannot expect these equations to hold when the scale of the motions is as small as a typical void in the porous bed. Despite this some of the experiments (figure 8) do seem to be consistent with the requirements of the dimensional arguments in the limit of large R.

It is appropriate, however, to compare the prediction of the dimensional argument with the variational arguments since these both assume that the DOB equations govern the motion when R is large.

To treat the variational problem at large R (or large μ or p) we followed the analysis of Chan (1971) in all essential details. The boundary-layer analysis is

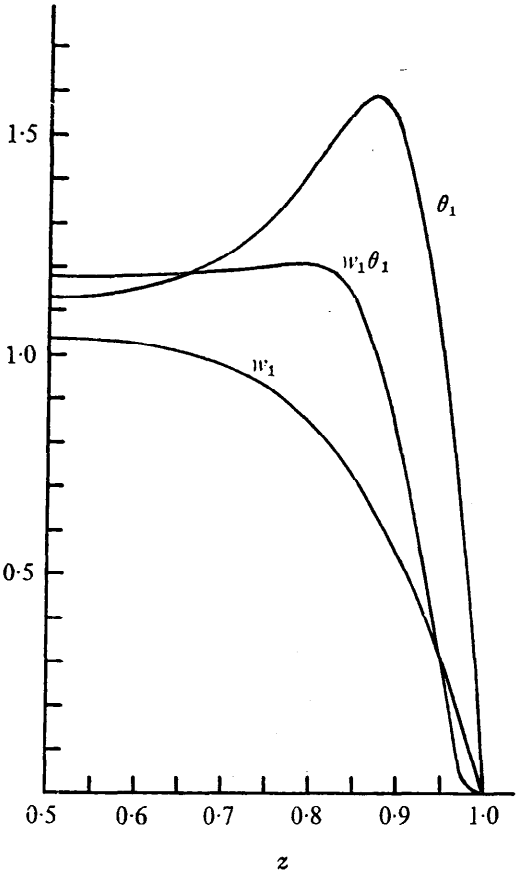

FIGURE 4. The single-α solutions when $p = 2000$ ($R = 207{\cdot}4$). A pronounced boundary-layer structure with $w_1\theta_1 \approx 1$ in the interior has not yet developed.

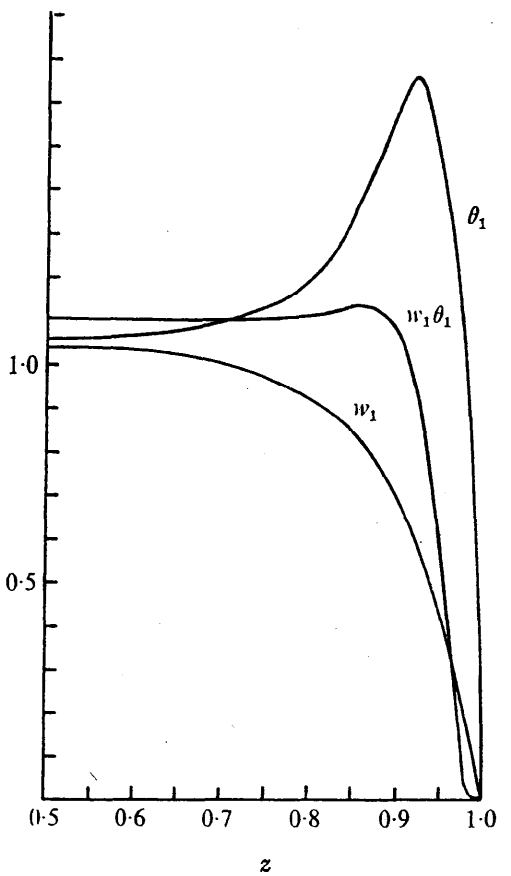

FIGURE 5. The single-α solutions when $p = 6000$ ($R = 382{\cdot}1$). A boundary-layer structure with $w_1\theta_1 \approx 1$ in the interior has developed. The $w_1\theta_1$ boundary layer is pushed closer to the wall by the overshoot of θ_1.

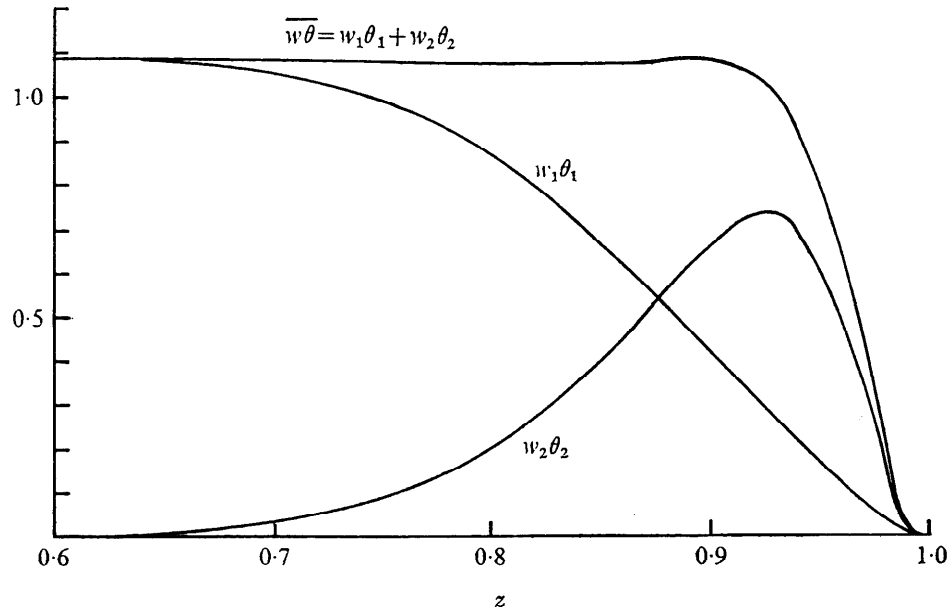

FIGURE 6. The two-α solution when $p = 8000$ ($R = 428{\cdot}7$). Here the boundary layer is such that $\overline{w\theta} = w_1\theta_1 + w_2\theta_2 \simeq 1$ at interior points. This boundary-layer structure is already fairly well developed.

based on the hypothesis that, when μ is large, $\overline{w\theta} = \sum_{i=1}^{N} w_i\theta_i = 1$ everywhere but in a small region of the boundary. This is a boundary layer in $\overline{w\theta}$ rather than in the separate factors w_i and θ_i. This kind of structure is already evident in figures 4, 5 and 6. Only the results of this analysis will be given here and we refer the reader to Gupta's thesis for details. We define $F^{[N]}$ to be the upper bound corresponding to a solution with N wavenumbers and find that

$$F^{[N]} = \left(\frac{2}{I}\right)^{\frac{4}{3}} (2{\cdot}3^N - 1)^{3^{-N}-2} \left(\frac{4}{\beta}\right)^{\frac{2}{3}(1-3^{-N+1})} (3)^{\frac{3}{2}N - \frac{11}{4}(1-3^{-N})} (R\ln^{\frac{1}{2}} R)^{1-3^{-N}}, \quad (8.1)$$

where

$$I = 2^{-\frac{1}{2}}\Gamma^2(\tfrac{3}{4}) \simeq 1{\cdot}062, \quad \beta = 64(12)^{\frac{1}{2}}/45 \simeq 2{\cdot}647,$$

and

$$\alpha_n = b_n R^{[1-\frac{3}{2}(\frac{1}{3})^n]} \prod_{k=1}^{n-1} \left(\frac{\ln R}{3^k}\right)^{\frac{1}{2}(\frac{1}{3})^{n-k}}, \quad (8.2)$$

where

$$b_1^2 = 1/[2 \times 3^N - 1] \quad (8.3)$$

and

$$b_{n+1} = 3^{n-\frac{3}{2}+\frac{1}{2}(\frac{1}{3})^{n-1}} (4/\beta)^{1-3^{-n}} b_1^{2-3^{-n}}. \quad (8.4)$$

Putting $N = 1$, 2 and 3 in (8.1) we get

$$\left.\begin{aligned} F^{[1]} &\simeq 0{\cdot}1103(R\ln^{\frac{1}{2}} R)^{\frac{2}{3}}, \\ F^{[2]} &\simeq 0{\cdot}2439 \times 10^{-1}(R\ln^{\frac{1}{2}} R)^{\frac{8}{9}}, \\ F^{[3]} &\simeq 0{\cdot}9370 \times 10^{-2}(R\ln^{\frac{1}{2}} R)^{\frac{26}{27}}. \end{aligned}\right\} \quad (8.5)$$

We note that $F^{[1]} = F^{[2]}$ at $R = R_{12} \cong 366{\cdot}4$.

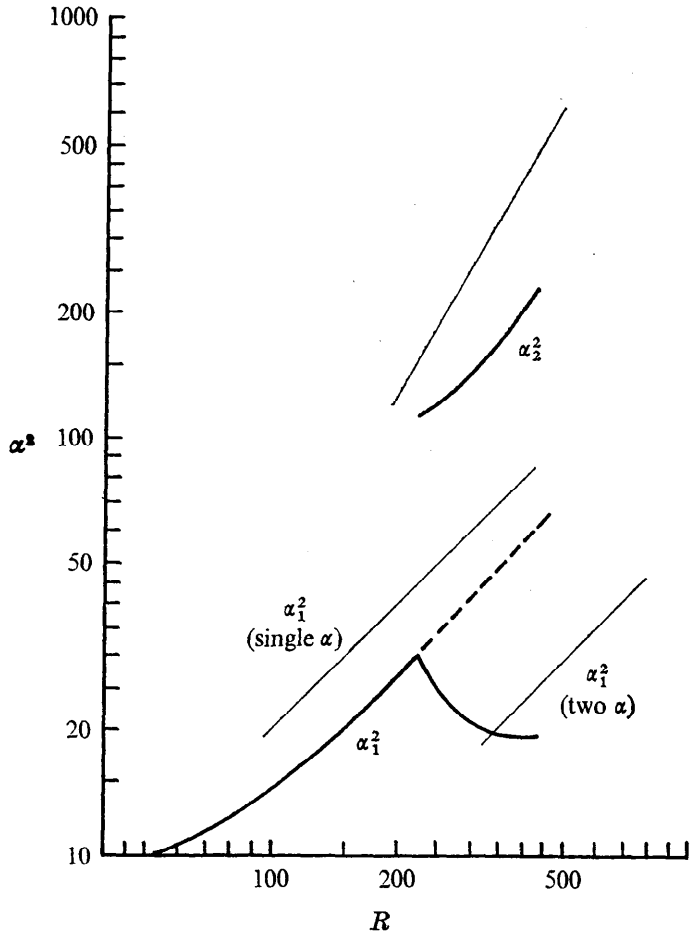

FIGURE 7. The variation of the optimizing wavenumbers. ——, two-α result; – –, continuation of the single-α solution past the point of bifurcation; ——, calculated from the boundary-layer theory.

The bounding Nusselt number is maximized by the single-α solution when $R < R_{12}$ and by the two-α solution when $R > R_{12}$. Recall that the exact value of R_{12} from numerical analysis is $R_{12} = 221{\cdot}5$. An analogous exchange in the minimizing properties of the solution occurs at $R_{23} = 1{\cdot}188 \times 10^5$ and so on. At each point of bifurcation a new solution with one more wavenumber maximizes Nu. Finally in the limit $N \to \infty$ we find that

$$F^{[\infty]} \cong Nu^{[\infty]} = 0{\cdot}01601R. \tag{8.6}$$

Graphs of equations (8.2)–(8.4) for the two-α solution are shown in figure 7. The graphs of (8.5) and (8.6) are shown in figure 8. The following three points deserve emphasis.

(*a*) The prediction of the dimensional argument on the slope of the heat-transport curve is supported by the result (8.6) of asymptotic analysis of the variational problem.

(*b*) Asymptotic results for $N = 1$ and $N = 2$ do not compare well quantitatively with the corresponding numerical results even though they become parallel on a log–log scale. It would appear from our numerical work that the basic ideas of the boundary-layer analysis are at least qualitatively correct; however, the

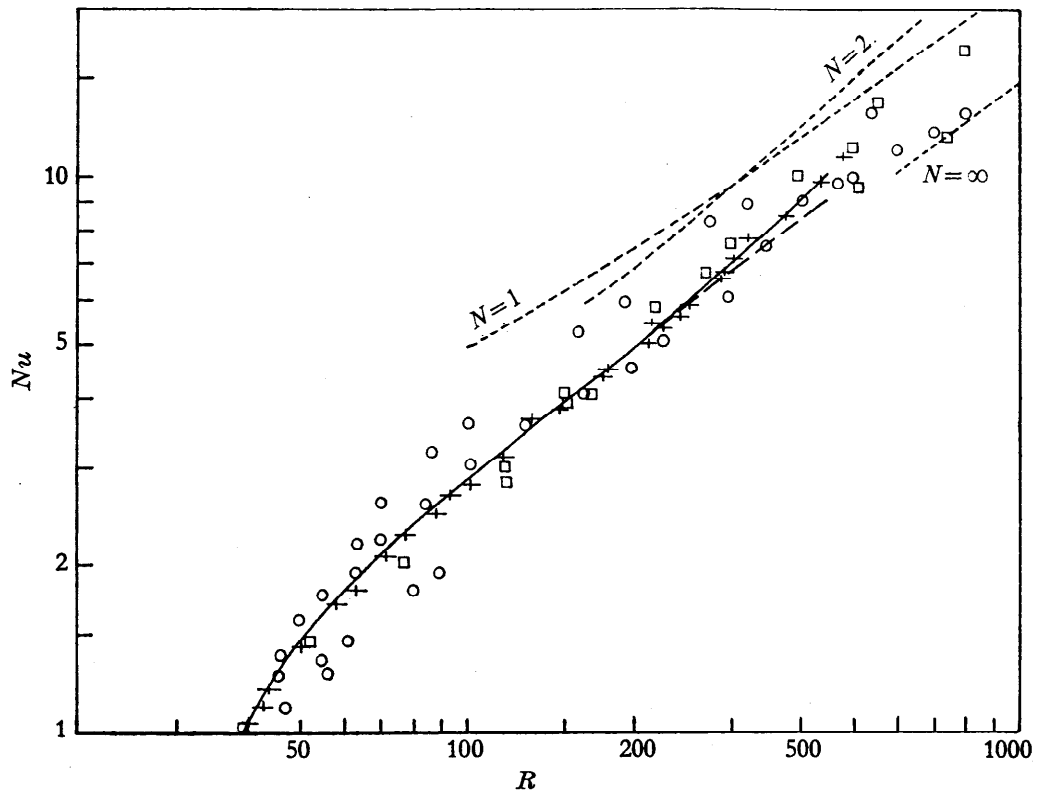

FIGURE 8. Compilation of published experimental data for convection in a porous layer heated from below. ——, two-α upper bound; – –, asymptotic results; ○, Combarnous & LeFur (1969); □, Elder (1967); +, Buretta & Berman. Schneider's (1963) data is like that shown but has more scatter in the region below the upper bound.

apparent discrepancy in the magnitudes of the variation of the parameters with R may mean that the boundary-layer analysis is not completely correct.

(*c*) The condition of infinite Prandtl–Darcy number ($B^{-1} = \infty$) which is explored in this paper leads to results which differ substantially from those which hold when this condition is relaxed. To establish this it suffices to draw attention to discrepancy in the results of this analysis, where we assume $B = 0$, and the analysis given in BJ, where no restriction on the value of B is imposed. In the analysis given in BJ the successive bifurcations of the Euler equations lead the upper bound far away from the data; ultimately, as $N \to \infty$, the bounding curve becomes proportional to e^R rather than R.

A similar improvement in the upper bound has been derived by Chan in his asymptotic analysis of infinite Prandtl number convection in a fluid layer.

This paper is based on the Ph.D. thesis of V. P. Gupta at the University of Minnesota. The work was partially supported under the NSF grant GK-12500.

REFERENCES

BEAVERS, G. & SPARROW, E. 1969 Non-Darcy flow through fibrous porous media. *J. Appl. Mech.* **36**, 711–714.

BELLMAN, R. E. & KALABA, R. E. 1965 *Modern Analytical and Computational Methods in Science and Mathematics.* Elsevier.

BURETTA, R. & BERMAN, A. S. 1973 Convective heat transfer in a liquid-saturated porous layer. (To appear.)

BUSSE, F. 1969 On Howard's upper bound for heat transport in turbulent convection. *J. Fluid Mech.* **37**, 457.

BUSSE, F. & JOSEPH, D. D. 1972 Bounds for heat transport in a porous layer. *J. Fluid Mech.* **54**, 521.

CHAN, S. 1971 Infinite Prandtl number turbulent convection. *Studies in Appl. Math.* **50** (1), 13–49.

COMBARNOUS, M. & LEFUR, B. 1969 Transfert de chaleur par convection naturelle dans une couche poreuse horizontale. *Comptes Rendus*, **269**, 1009–1012.

CONTE, S. D. 1966 The numerical solution of linear boundary value problems. *SIAM Rev.* **8**, 309.

ELDER, J. W. 1967 Steady free convection in a porous medium heated from below. *J. Fluid Mech.* **27**, 29–48.

FIFE, P. & JOSEPH, D. D. 1969 Existence of convective solutions of the generalized Bénard problem which are analytic in their norm. *Arch. Rat. Mech. Anal.* **33**, 116–138.

FORCHHEIMER, P. H. 1901 Wasserbewegun durch Boden. *Z. ver. dtsch. Ing.* **45**, 1782–1788.

GUPTA, V. P. 1972 Upper bound on heat transfer across a porous fluid layer heated from below. Ph.D. thesis, University of Minnesota.

HEINRICI, P. 1964 *Elements of Numerical Analysis.* Wiley.

HOWARD, L. N. 1963 Heat transport in turbulent convection. *J. Fluid Mech.* **17**, 405–432.

IRMAY, S. 1958 On the theoretical derivation of Darcy and Forchheimer formulas. *Trans. Am. Geophys. Un.* **39**, 702–707.

JOSEPH, D. D. & SATTINGER, D. H. 1972 Bifurcating time periodic solutions and their stability. *Arch. Rat. Mech. Anal.* **45**, 79–109.

KRISHNAMURTI, R. 1970*a* On the transition to turbulent convection. Part 1. *J. Fluid Mech.* **42**, 295.

KRISHNAMURTI, R. 1970*b* On the transition to turbulent convection. Part 2. *J. Fluid Mech.* **42**, 309.

LAPWOOD, E. R. 1948 Convection of a fluid in a porous medium. *Proc. Camb. Phil. Soc.* **44**, 508–521.

MALKUS, W. V. R. 1954*a* Discrete transitions in turbulent convection. *Proc. Roy. Soc.* A **225**, 185.

MALKUS, W. V. R. 1954*b* The heat transport and spectrum of thermal turbulence. *Proc. Roy. Soc.* A **225**, 196.

SCHNEIDER, K. J. 1963 Investigation of the influence of free thermal convection on heat transfer through granular material. *11th Int. Cong. of Refrigeration (Munich), paper*, 11-4.

SCHMIDT, R. J. & SAUNDERS, O. A. 1938 On the instability of a fluid when heated from below. *Proc. Roy. Soc.* A **165**, 216.

WARD, J. C. 1964 Turbulent flow in porous media. *J. Hydraul. Div., Proc. A.S.C.E.* **90** (HY5), 1–12.

WESTBROOK, D. R. 1969 The stability of convective flow in a porous medium. *Phys. Fluids*, **12**, 1547.